



**HAL**  
open science

## **In vitro blood–brain barrier permeability predictions for GABAA receptor modulating piperine analogs**

Daniela Elisabeth Eigenmann, Carmen Dürig, Evelyn Andrea Jähne, Martin Smieško, Maxime Culot, Fabien Gosselet, Roméo Cecchelli, Hans Christian Cederberg Helms, Birger Brodin, Laurin Wimmer, et al.

### ► **To cite this version:**

Daniela Elisabeth Eigenmann, Carmen Dürig, Evelyn Andrea Jähne, Martin Smieško, Maxime Culot, et al.. In vitro blood–brain barrier permeability predictions for GABAA receptor modulating piperine analogs. *European Journal of Pharmaceutics and Biopharmaceutics*, 2016, 103, pp.118-126. 10.1016/j.ejpb.2016.03.029 . hal-02510088

**HAL Id: hal-02510088**

**<https://univ-artois.hal.science/hal-02510088>**

Submitted on 9 Jul 2022

**HAL** is a multi-disciplinary open access archive for the deposit and dissemination of scientific research documents, whether they are published or not. The documents may come from teaching and research institutions in France or abroad, or from public or private research centers.

L'archive ouverte pluridisciplinaire **HAL**, est destinée au dépôt et à la diffusion de documents scientifiques de niveau recherche, publiés ou non, émanant des établissements d'enseignement et de recherche français ou étrangers, des laboratoires publics ou privés.

## ***In vitro* blood-brain barrier permeability predictions for GABA<sub>A</sub> receptor modulating piperine analogs**

Daniela Elisabeth Eigenmann<sup>a</sup>, Carmen Dürig<sup>a</sup>, Evelyn Andrea Jähne<sup>a</sup>, Martin Smieško<sup>b</sup>, Maxime Culot<sup>c</sup>, Fabien Gosselet<sup>c</sup>, Romeo Cecchelli<sup>c</sup>, Hans Christian Cederberg Helms<sup>d</sup>, Birger Brodin<sup>d</sup>, Laurin Wimmer<sup>e</sup>, Marko D. Mihovilovic<sup>e</sup>, Matthias Hamburger<sup>a</sup>, and Mouhssin Oufir<sup>a,\*</sup>

<sup>a</sup>Pharmaceutical Biology, Department of Pharmaceutical Sciences, University of Basel, Klingelbergstrasse 50, CH-4056 Basel, Switzerland

<sup>b</sup>Molecular Modeling, Department of Pharmaceutical Sciences, University of Basel, Klingelbergstrasse 50, CH-4056 Basel, Switzerland

<sup>c</sup>Univ. Artois, EA 2465, Laboratoire de la Barrière Hémato-Encéphalique (LBHE), F-62300 Lens Cedex, France

<sup>d</sup>Drug Transporters in ADME, Department of Pharmacy, Faculty of Health and Medical Sciences, University of Copenhagen, Universitetsparken 2, DK-2100 Copenhagen, Denmark

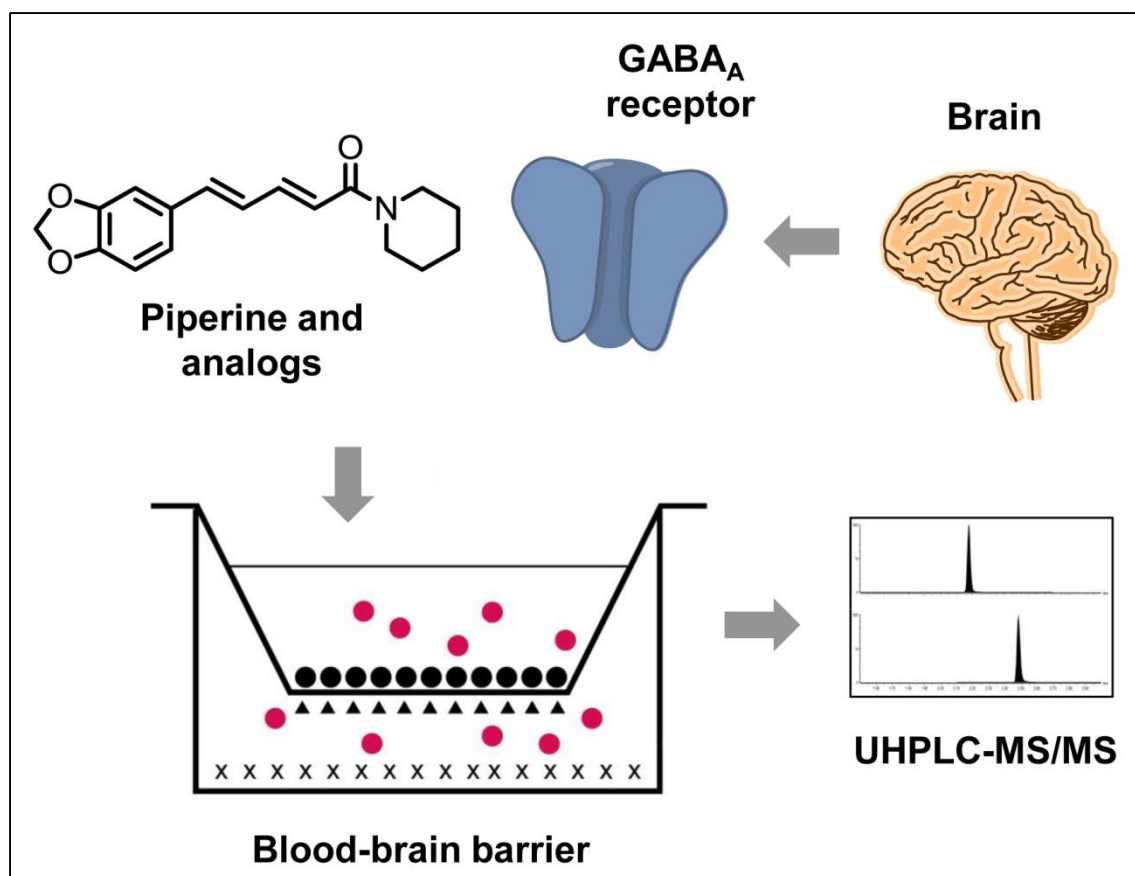
<sup>e</sup>Institute of Applied Synthetic Chemistry, TU Wien, Getreidemarkt 9, A-1060 Vienna, Austria

\*Corresponding author. Pharmaceutical Biology, Department of Pharmaceutical Sciences, University of Basel, Klingelbergstrasse 50, CH-4056 Basel, Switzerland. Tel: +41 61 2671425; fax: +41 61 2671474.

E-mail address: mouhssin.oufir@unibas.ch (M. Oufir).

**Keywords:** Piperine, GABA<sub>A</sub> receptor, *in vitro* blood-brain barrier (BBB) model, primary cells, immortalized cell line, human stem cells, UHPLC-MS/MS, permeability coefficient, *in silico* prediction

**Abbreviations:** BBB, blood-brain barrier; BLEC, human brain-like endothelial cells; BSA, bovine serum albumin; C<sub>CL</sub>, cell layer capacitance; CNS, central nervous system; CV, coefficient of variation; DMEM, Dulbecco's Modified Eagle Medium; ER, efflux ratio; FA, formic acid; FBS, fetal bovine serum; GABA<sub>A</sub> receptor,  $\gamma$ -aminobutyric acid type A receptor; hBMEC, human brain microvascular endothelial cell line; I.S., internal standard; LLOQ, lower limit of quantification; MRM, multiple reaction monitoring; Na-F, sodium fluorescein; P<sub>app</sub>, apparent permeability coefficient; P<sub>e</sub>, endothelial permeability coefficient; P-gp, P-glycoprotein; QC, quality control; RE, relative error; RHB, Ringer HEPES buffer; TEER, transendothelial electrical resistance; TRPV1, transient receptor potential vanilloid 1; UHPLC-MS/MS, ultra-high performance liquid chromatography tandem mass spectrometry; ULOQ, upper limit of quantification.



## Abstract

The alkaloid piperine from black pepper (*Piper nigrum* L.) and several synthetic piperine analogs were recently identified as positive allosteric modulators of  $\gamma$ -aminobutyric acid type A (GABA<sub>A</sub>) receptors. In order to reach their target sites of action, these compounds need to enter the brain by crossing the blood-brain barrier (BBB). We here evaluated piperine and five selected analogs (SCT-66, SCT-64, SCT-29, LAU397, and LAU399) regarding their BBB permeability. Data were obtained in three *in vitro* BBB models, namely a recently established human model with immortalized hBMEC cells, a human brain-like endothelial cells (BLEC) model, and a primary animal (bovine endothelial/rat astrocytes co-culture) model. For each compound, quantitative UHPLC-MS/MS methods in the range of 5.00–500 ng/mL in the corresponding matrix were developed, and permeability coefficients in the three BBB models were determined. *In vitro* predictions from the two human BBB models were in good agreement, while permeability data from the animal model differed to some extent, possibly due to protein binding of the screened compounds. In all three BBB models, piperine and SCT-64 displayed the highest BBB permeation potential. This was corroborated by data from *in silico* prediction. For the other piperine analogs (SCT-66, SCT-29, LAU397, and LAU399), BBB permeability was low to moderate in the two human BBB models, and moderate to high in the animal BBB model. Efflux ratios (ER) calculated from bidirectional permeability experiments indicated that the compounds were likely not substrates of active efflux transporters.

## 1 Introduction

The alkaloid piperine, the major pungent component of black pepper (*Piper nigrum* L.), was recently identified as a positive allosteric  $\gamma$ -aminobutyric acid type A (GABA<sub>A</sub>) receptor modulator. The compound showed anxiolytic-like activity in behavioral mouse models, and was found to interact with the GABA<sub>A</sub> receptors at a binding site that was independent of the benzodiazepine binding site [1,2]. Given that the compound complied with Lipinski's "rule of five" [1], it represented a new scaffold for the development of novel GABA<sub>A</sub> receptor modulators [1–3].

Given that piperine also activates the transient receptor potential vanilloid 1 (TRPV1) receptors [4] which are involved in pain signaling and regulation of the body temperature [5,6], structural modification of the parent compound was required to dissect GABA<sub>A</sub> and TRPV1 activating properties.

In a first step, the piperidine ring of piperine was replaced by a *N,N*-diisobutyl residue, resulting in a non-TRPV1 activating derivative (designated as SCT-66) (Fig. 1) [2]. Compared to piperine, SCT-66 increased chloride currents through GABA<sub>A</sub> receptors more potently and efficiently, and showed a stronger anxiolytic effect in mice [7]. Based on these findings, a library of 76 piperine analogs with modifications at the amide functionality and at the linker region was synthesized [7]. In this compound series, SCT-64 and SCT-29 (Fig. 1) showed the strongest modulation and highest potency, respectively, at GABA<sub>A</sub> receptors expressed in *Xenopus laevis* oocytes [7]. Both analogs were devoid of TRPV1 receptor activating properties *in vitro*, exerted pronounced anxiolytic effects in mice, and appeared in significant concentration in mouse plasma after intraperitoneal application [7]. However, all compounds synthesized up to that point contained the metabolically liable 1,3-benzodioxole group [8]. Hence, a set of 15 aryl-modified piperine analogs was synthesized bearing the non-natural dibutylamide function [9]. Of these, the analogs LAU397 and LAU399 (Fig. 1) were significantly more efficient at the GABA<sub>A</sub> receptor than piperine while being devoid of *in vitro* TRPV1 receptor interaction [9].

For drugs acting on the central nervous system (CNS), brain penetration is required. This process is controlled by the blood-brain barrier (BBB), a tight layer of endothelial cells lining the brain capillaries that limits the passage of molecules from the blood circulation into the brain [10]. Since low BBB permeability can reduce CNS exposure [11], lead compounds should be evaluated at an early stage of the drug development process for their ability to permeate the BBB [12].

In the present study, we assessed the BBB permeability of piperine and five selected piperine analogs (Fig. 1) in three *in vitro* cell-based BBB models, namely a recently established human model with immortalized hBMEC cells, a human brain-like endothelial cells (BLEC) model, and a primary animal (bovine endothelial/rat astrocytes co-culture) model [13–17]. Permeability coefficients across the cell monolayers were determined by means of UHPLC-MS/MS, whereby quantitative UHPLC-MS/MS assays in the corresponding matrix were developed for each compound. In addition, we calculated descriptors relevant for BBB permeation and compared them with the *in vitro* data from the BBB models.

## 2 Materials and methods

### 2.1 Chemicals and reagents

The piperine analogs (2*E*,4*E*)-5-(benzo[*d*][1,3]dioxol-5-yl)-*N,N*-diisobutylpenta-2,4-dienamide (SCT-66), (2*E*,4*E*)-5-(benzo[*d*][1,3]dioxol-5-yl)-*N,N*-dipropylpenta-2,4-dienamide (SCT-64), (2*E*,4*E*)-5-(benzo[*d*][1,3]dioxol-5-yl)-*N,N*-dibutylpenta-2,4-dienamide (SCT-29), (2*E*,4*E*)-*N,N*-dibutyl-5-(4-methoxyphenyl)penta-2,4-dienamide (LAU397; compound 6 in reference [9]), and (2*E*,4*E*)-*N,N*-dibutyl-5-(thiophen-3-yl)penta-2,4-dienamide (LAU399; compound 16 in reference [9]) were synthesized at TU Wien as described elsewhere [2,7,9]. Piperine, Tween 20, bovine serum albumin (BSA), Dulbecco's Modified Eagle Medium (DMEM) high glucose, and sodium fluorescein (Na-F) were purchased from Sigma-Aldrich (Steinheim, Germany). Fetal bovine serum (FBS) was from Pan-Biotech (Aidenbach, Germany). Immortalized human brain microvascular cell line (hBMEC) [13] was received from Prof. Kwang Sik Kim and Prof. Dennis Grab (Johns Hopkins University, Baltimore, MD, USA). Acetonitrile, formic acid (FA), and ammonium formate were all HPLC grade and were obtained from BioSolve (Valkenswaard, the Netherlands). HPLC grade water was obtained by a Milli-Q integral water purification system (Millipore Merck, Darmstadt, Germany). Ringer HEPES buffer (RHB) (150 mM NaCl, 2.2 mM CaCl<sub>2</sub>, 0.2 mM MgCl<sub>2</sub>, 5.2 mM KCl, 2.8 mM glucose, 5 mM HEPES, 6 mM NaHCO<sub>3</sub>) was prepared in-house, adjusted to pH 7.4, filtered, and stored at 4°C.

### 2.2 Stock solutions, calibration standards, and quality controls

Stock solutions and working solutions of analytes and internal standard (I.S.) were prepared as described elsewhere [15]. For all compounds, calibration standards (calibrators) in the range of 5.00–500 ng/mL (5.00, 25.0, 50.0, 100, 200, 400, and 500 ng/mL) and quality controls (QCs) at low, middle, and high concentration (QCL: 15.0 ng/mL, QCM: 250 ng/mL, and QCH: 400 ng/mL) were prepared in modified RHB (RHB + 0.2% Tween 20) and modified DMEM (DMEM + 10% FBS for piperine, LAU397, and LAU399; DMEM + 10% FBS + 0.2% Tween 20 for the other analogs) by serial dilution of the respective working solutions. The lowest concentration level of the calibrators was defined as lower limit of quantification (LLOQ), and the highest level as upper limit of quantification (ULOQ).

### 2.3 Sample extraction

Prior to sample injection into the UHPLC-MS/MS system, analytes and I.S. were extracted from the matrices by means of protein precipitation.

**Samples in modified RHB:** Sample aliquots in modified RHB (100 µL; exception LAU399: 200 µL) were spiked with a freshly prepared working solution (between 200–1000 ng/mL) of the corresponding I.S. (100 µL) (Table S1). Samples were subsequently spiked with 200 µL BSA solution (60 g/L) and subjected to protein precipitation with ice cold acetonitrile (1000 µL). After vortexing and stirring for 10 min on an Eppendorf Mixmate (Vaudaux-Eppendorf, Schönenbuch, Switzerland), the mixture was centrifuged for 20 min at 13200 rpm (MiniSpin plus, Vaudaux-Eppendorf). The supernatant (1200 µL) was transferred into a 96-deep well plate (96-DWP), dried under nitrogen (Evaporex EVX-96, Apricot Designs, Monrovia, CA, USA) and reconstituted with injection solvent (65% mobile phase A and 35% mobile phase B, v/v). Prior to injection (5 µL) into the UHPLC, the 96-DWP was stirred on an Eppendorf Mixmate for 30 min at 2000 rpm and then centrifuged for 4 min at 3000 rpm (Megafuge, Heraeus Instruments AG, Switzerland).

***Samples in modified DMEM:*** Sample aliquots in modified DMEM (100  $\mu$ L) were spiked with a freshly prepared working solution (between 200–1000 ng/mL) of the corresponding I.S. (100  $\mu$ L) (Table S1) and directly subjected to protein precipitation by the addition of ice cold acetonitrile (1000  $\mu$ L). After vortexing and stirring for 10 min on an Eppendorf Mixmate, the mixture was centrifuged for 20 min at 13200 rpm. The supernatant (1000  $\mu$ L) was thereafter transferred into a 96-DWP. The subsequent procedure was the same as described above.

#### **2.4 UHPLC-MS/MS settings**

Method development was performed on a 1290 Infinity UHPLC system coupled to a 6460 Triple Quadrupole mass spectrometer (all Agilent, Waldbronn, Germany). Data were acquired and quantification was done using MassHunter version B.07.00 (Agilent). Separation was performed on a Kinetex PFP column (particle size 1.7  $\mu$ m, 2.1 x 50 mm) (Phenomenex, Torrance, CA, USA) heated to 55°C. Mobile Phase A was 10 mM ammonium formate containing 0.05% FA, and mobile phase B was acetonitrile containing 0.05% FA. The flow rate was set at 0.5 mL/min. The gradient started at 1 min with 40% of B and increased to 70% of B within 3.00 min, followed by a column washing step with 100% of B for 1 min. Measurements were performed in electrospray ionization positive ion mode (ESI+) and multiple reaction monitoring (MRM) mode. MS/MS parameters were as follows: drying gas (nitrogen) temperature and flow rate were 320°C and 10 L/min, respectively, nebulizer pressure was 20 psi, sheath gas temperature was 400°C (300°C for LAU399 in modified DMEM), and flow rate was 11 L/min (6 L/min for LAU399 in modified DMEM). Capillary voltage was 2500 V (3500 V for LAU399 in modified DMEM). MRM transitions, fragmentor voltage, and collision energy for each compound are listed in Table S1.

#### **2.5 Analytical runs**

##### ***Calibration curve and regression analysis***

Each analytical run consisted of a set of seven calibrators injected with increasing concentration after a blank sample (blank matrix) and a calibrator zero (blank matrix only spiked with I.S.) at the beginning and at the end of the run. A calibration curve was considered valid if the coefficient of determination ( $R^2$ ) was higher than 0.96 and if at least 75% of all calibrators were used to generate the calibration curve. The back calculated concentrations of the calibrators had to be within  $\pm 15\%$  of the nominal values at all concentration levels (exception LLOQ: within  $\pm 20\%$ ). For the LLOQ and ULOQ, at least one replicate had to be accepted. The calibration curve was validated through six QCs (duplicates of QCL, QCM, and QCH), which were inserted randomly into the analytical run. The back calculated concentrations had to be within  $\pm 15\%$  of the nominal values at all QC levels. For the six QCs, at least four replicates in total and at least one replicate at each concentration level had to be accepted. Imprecision in all analytical runs was expressed by the coefficient of variation (CV %), and had to be below 15% (below 20% at the LLOQ) of the nominal values at all concentration levels. Inaccuracy was expressed by the relative error (RE %), and had to be within  $\pm 15\%$  (within  $\pm 20\%$  at the LLOQ) of the nominal values at all concentration levels [18,19].

##### ***Carry-over***

To assess the carry-over of both analyte and I.S. in each analytical run, blank samples were injected after both replicates of the ULOQ. Peak areas of analyte and I.S. in these blank samples were then compared to the peak

areas at the LLOQ. Mean carry-over in each analytical run, expressed in %, had to be below 20% for analytes, and below 5% for I.S. [19].

### ***Between-run reproducibility***

Between-run reproducibility was assessed by calculating the imprecision (CV %) and inaccuracy (RE %) at five concentration levels (LLOQ, QCL, QCM, QCH, and ULOQ) of two replicates injected within three analytical runs on three different days (n = 6).

## **2.6 *In vitro* BBB models**

***Immortalized in vitro human BBB model:*** The immortalized human mono-culture *in vitro* BBB model based on hBMEC cell line [13] was prepared as reported previously [14,15]. Tissue culture inserts (24-well format) were from Greiner Bio-one (0.336 cm<sup>2</sup>, transparent PET membrane, 3.0 µm pore size, Greiner Bio-one, Frickenhausen, Germany), and were coated with rat tail collagen I. The permeability experiments were carried out bidirectionally (i.e. in the apical-to-basolateral (A→B) and basolateral to apical (B→A) direction), with working solutions containing the test compound (2 µM) and Na-F (10 µg/mL) in RHB + 0.1% BSA. Aliquots of donor and receiver compartments were collected after several time points (15, 30, 60, and 120 min) (one insert per time point).

***In vitro human brain-like endothelial cells (BLEC) BBB model:*** The human *in vitro* BBB model derived from hematopoietic stem cells was prepared as described previously [16]. Tissue culture inserts (12-well format) were from Corning (1.12 cm<sup>2</sup>, polycarbonate membrane, 0.4 µm pore size, Corning, New York, USA), and were coated with matrigel. The permeability experiments were carried out bidirectionally, with working solutions containing the test compound (2 µM) and Na-F (10 µg/mL) in RHB + 0.1% BSA. After 15, 30, and 60 min for A→B transport, inserts were transferred into a new receiver well plate filled with transport buffer. After 15, 30, 60, and 120 min for A→B transport (or after 120 min incubation for B→A), an aliquot from each donor and receiver compartment was withdrawn.

***In vitro primary bovine endothelial/rat astrocytes co-culture BBB model:*** The bovine endothelial/rat astrocytes co-culture model was prepared as described previously [17]. Tissue culture inserts (12-well format) were from Corning (1.12 cm<sup>2</sup>, polycarbonate membrane, 0.4 µm pore size, Corning, New York, USA), and were coated with collagen/fibronectin. The permeability experiments were carried out bidirectionally, with working solutions containing the test compound (5 µM) and Na-F (10 µg/mL) in DMEM + 10% FBS. Aliquots were withdrawn from the receiver compartments after 15, 30, 60, and 120 min, and from the donor compartment after 120 min.

All experiments were performed at least in triplicate. Withdrawn samples were stored below -65°C. Before UHPLC-MS/MS analysis, samples were diluted with an equal volume of the corresponding matrix containing 0.4% Tween 20 in order to avoid non-specific adsorption to surfaces.

## **2.7 Calculation of permeability coefficients**

For the two human *in vitro* BBB models, endothelial permeability coefficients ( $P_e$ ) for each test compound and for Na-F were calculated as follows. For each replicate (control inserts without cells and inserts with cells), the clearance was calculated according to the following equation [20,21]:

$$\text{Clearance } (\mu\text{L}) = C_R V_R / C_D \quad (1)$$

where  $C_R$  and  $V_R$  are the concentration and volume in the receiver compartments, respectively, and  $C_D$  is the initial concentration in the donor compartment. The mean cleared volume was plotted as a function of time (15, 30, 60, and 120 min), and the slope was estimated by linear regression analysis. Permeability-surface area products (PS) and  $P_e$  values were subsequently calculated according to the following equations [20,21]:

$$1/PS_{\text{total}} - 1/PS_{\text{filter}} = 1/PS_e \quad (2)$$

$$PS_e/A = P_e \text{ (cm/s)} \quad (3)$$

where  $PS_{\text{total}}$  is the slope of the clearance curve of cell monolayers with filter inserts,  $PS_{\text{filter}}$  is the slope of the clearance curve of control filter inserts without cells,  $PS_e$  is the slope of the clearance curve of the endothelial monolayers, and  $A$  is the surface area of the filter membrane.

For all three models, apparent permeability coefficients ( $P_{\text{app}}$ ) were calculated according to the following equation [22,23]:

$$P_{\text{app}} \text{ (cm/s)} = J/(AC_D) \quad (4)$$

where  $J$  is the rate of appearance of the compounds in the receiver compartment,  $A$  is the surface area of the filter membrane, and  $C_D$  is the initial concentration in the donor compartment.

Furthermore, efflux ratios (ER) were calculated:

$$ER = P_{\text{app}} \text{ (B} \rightarrow \text{A)} / P_{\text{app}} \text{ (A} \rightarrow \text{B)} \quad (5)$$

where  $P_{\text{app}} \text{ (B} \rightarrow \text{A)}$  and  $P_{\text{app}} \text{ (A} \rightarrow \text{B)}$  are the  $P_{\text{app}}$  values in the direction basolateral-to-apical and apical-to-basolateral, respectively. A high ER indicates a potentially significant role for efflux transporters in the passage of a compound across cell monolayers. Compounds with a  $ER > 2$  are thus usually categorized as efflux transporter substrates [24,25].

Recovery (mass balance) of each compound was calculated according to the following equation:

$$\text{Recovery } (\%) = (N_{Df} + N_{Rf}) / N_{Di} \times 100 \quad (6)$$

where  $N_{Df}$  and  $N_{Rf}$  are the final amounts of the compounds in the donor and receiver compartments, respectively, and  $N_{Di}$  is the initial amount in the donor compartment. All results are expressed as means  $\pm$  standard deviation (SD).

## 2.8 *In silico* prediction of BBB permeability

Three-dimensional computer models of studied compounds were built in Maestro modeling environment [26]. The global minimum geometry was used as an input for the QikProp application [27] to evaluate various descriptors relevant for compound permeability through the BBB. The polar surface area (PSA) and the logarithm of partition and distribution coefficient (LogP and LogD7.4, respectively) descriptors were calculated using the Calculator plugin of Chemaxon Marvin application [28].

## 3 Results

### 3.1 UHPLC-MS/MS

#### *Chromatographic performance*

Calibration curves in the range of 5.00–500 ng/mL for each analyte were fitted by least-squares quadratic regression, and a weighting factor of 1/X was applied. The mean coefficients of determination ( $R^2$ ) ranged from 0.9945 to 0.9996 (Tables S2 and S3).

### ***Carry-over***

Mean carry-over in blank matrix samples (modified RHB and modified DMEM) injected after the ULOQ were between 0.00% to 4.27% for analytes (below 20%), and between 0.00% and 0.0597% for I.S. (below 5%) (Table S4), indicating that carry-over did not have an impact on the results.

### ***Between-run reproducibility***

Between-run imprecision (CV %) was between 1.17% and 14.9% (below 15%), and between-run inaccuracy (RE %) was between -8.15% and 10.0% (within  $\pm 15\%$ ) at all calibration levels in both matrices (modified RHB and modified DMEM) (Tables S5 and S6), indicating that the methods were accurate, precise, and reproducible.

## **3.2 Immortalized *in vitro* human BBB model (based on hBMEC cell line)**

In the immortalized *in vitro* human BBB model [14,15], piperine showed a mean  $P_{e(A \rightarrow B)}$  value of  $53.7 \pm 4.47 \times 10^{-6}$  cm/s, indicating significant BBB permeability when compared to the mean  $P_{e(A \rightarrow B)}$  value of the negative control Na-F ( $6.51 \pm 0.163 \times 10^{-6}$  cm/s) (Fig. 2A, Table 1). SCT-64 and LAU399 showed lower mean  $P_{e(A \rightarrow B)}$  values ( $26.4 \pm 1.48 \times 10^{-6}$  cm/s and  $21.6 \pm 9.52 \times 10^{-6}$  cm/s, respectively) than piperine (Fig. 2A, Table 1), which were however still significantly higher than those for Na-F ( $4.50$  and  $4.83 \times 10^{-6}$  cm/s, respectively). Compounds SCT-66, SCT-29, and LAU397 showed mean  $P_{e(A \rightarrow B)}$  values between  $4.29$  and  $9.32 \times 10^{-6}$  cm/s (Fig. 2A, Table 1), suggesting low BBB permeability when compared to Na-F. The compounds could be ranked based on their  $P_{e(A \rightarrow B)}$  values in the following order: piperine > SCT-64/LAU399 > SCT-66 > LAU397/SCT-29. ER values for the compounds (except SCT-29) were between 0.750 and 1.92 (Table S7), suggesting that permeability of the compounds was not affected by active efflux transporters [24,25].

Mean transendothelial electrical resistance (TEER) values were between 20–40  $\Omega\text{cm}^2$  for the BBB drug permeability experiments, and were in the same range after the assays (Fig. S1). Mean cell layer capacitance ( $C_{CL}$ ) values were in the range of 0.5–5.0  $\mu\text{F}/\text{cm}^2$  (Fig. S1), indicating cell confluency of hBMEC monolayers and validating TEER values [29]. During the permeability assays,  $P_{app}$  values for Na-F were constant, indicating that barrier integrity of hBMEC monolayers was maintained throughout the experiments.

## **3.3 *In vitro* human brain-like endothelial cells (BLEC) BBB model**

In the *in vitro* human BLEC model [16], piperine, SCT-66, and SCT-64 showed mean  $P_{e(A \rightarrow B)}$  values between  $26.7$  and  $97.8 \times 10^{-6}$  cm/s (Fig. 2B, Table 2) that were indicative of moderate to high BBB permeability when compared to the mean  $P_{e(A \rightarrow B)}$  values for Na-F ( $9.99$ – $12.0 \times 10^{-6}$  cm/s). The analogs SCT-29, LAU397, and LAU399 showed mean  $P_{e(A \rightarrow B)}$  values between  $4.61$  and  $12.4 \times 10^{-6}$  cm/s (Fig. 2B, Table 2), suggesting low permeability when compared to Na-F. The compounds could be ranked regarding their  $P_{e(A \rightarrow B)}$  values as follows: piperine > SCT-66/SCT-64 > LAU397 > LAU399/SCT-29.

For all compounds (except piperine), mean recoveries were rather low (between 55.7% and 68.5%; Table 2), also in the absence of cells (data not shown). This was indicative of a possible non-specific binding of analytes to plastic surfaces and/or coating material of the inserts and transwell plates. Thus,  $P_{e(A \rightarrow B)}$  values might be underestimated.

ER values for all compounds were between 0.406 and 0.804 (Table S8), suggesting that the compounds were not substrates of active efflux. Mean TEER values, at which permeability experiments were carried out, were between 150–200  $\Omega\text{cm}^2$  [16].

### 3.4 *In vitro* primary bovine endothelial/rat astrocytes co-culture BBB model

In the primary bovine endothelial/rat astrocytes co-culture *in vitro* BBB model [17], the compounds showed mean  $P_{\text{app}(A \rightarrow B)}$  values between 20.9 and 81.3  $\times 10^{-6}$  cm/s (Fig. 2C, Table 3). Compared to the mean  $P_{\text{app}(A \rightarrow B)}$  values of Na-F (2.15–5.07  $\times 10^{-6}$  cm/s; Table 3), these values were considerably higher, indicating high BBB permeability for all compounds. The compounds could be ranked based on their  $P_{\text{app}(A \rightarrow B)}$  values in the following order: piperine > SCT-64 > LAU399/LAU397 > SCT-66/SCT-29.

However, the mean  $P_{\text{app}(A \rightarrow B)}$  values for Na-F in presence of the test compounds (2.15–5.07  $\times 10^{-6}$  cm/s; Table 3) were up to five times higher than those usually obtained in the model (below 1  $\times 10^{-6}$  cm/s). Mean  $P_{\text{app}}$  values in the direction B→A for Na-F in presence of the compounds, on the other hand, were in this expected range (below 1  $\times 10^{-6}$  cm/s; Table S9). Hence, a polarized opening of the paracellular space may have occurred when the compounds were applied on the apical side (but not on the basolateral side). For piperine, we further investigated this junctional effect by applying the compound separately to the apical and basolateral side of the inserts (at 5  $\mu\text{M}$ ), and measuring TEER as a function of incubation time. Throughout a two hour incubation period, the TEER was relatively stable for control cell monolayers and for cell monolayers to which piperine was applied on the basolateral side (Fig. 3). However, TEER values decreased from 1261 to 268  $\Omega\text{cm}^2$  for cell monolayers to which piperine was added on the apical side (Fig. 3), supporting the hypothesis of a polarized paracellular opening.

ER values for all compounds were between 0.340 and 0.584 (Table S9), indicating no involvement of active efflux transporters. TEER values, at which experiments were performed, were in the range of 1900–2500  $\Omega\text{cm}^2$ .

### 3.5 *In silico* prediction of BBB permeability

The analysis of descriptors relevant for the BBB permeation showed that the compounds had a PSA (26.9–48.1  $\text{\AA}^2$ ; Table 4) below the recommended thresholds of 70  $\text{\AA}^2$  [30] and 90  $\text{\AA}^2$  [31], which favors their passive permeation across the BBB. Similarly, their molecular weight (MW) was below the recommended value of 450 g/mol for CNS drugs (between 285 and 329 g/mol; Table 4) [31]. All compounds had a low effective number of H-bond acceptors (< 5) and no H-bond donors (Table 4), which facilitates their desolvation before entering into the lipophilic phase of the cell membranes. The QikProp model for brain/blood partitioning predicted favorable LogBB parameters (between -0.51 and -0.12) for all compounds (for 95% of known drugs, values range between -3.0 and 1.2), and the predicted permeability across Madin-Darby Canine Kidney (MDCK) and Caco-2 cells was

very high ( $> 2000$  nm/s; Table 4). LogP values for the compounds ranged from 3.27 to 5.34 (recommended values for CNS drugs are between 1–4), and the total numbers of rotatable bonds were between 3 and 10 (Table 4) (less than 6 rotatable bonds recommended for CNS drugs [32]).

#### 4 Discussion

The alkaloid piperine was recently identified as a promising lead compound for the development of positive allosteric GABA<sub>A</sub> receptor modulating drugs interacting at an up to now poorly characterized binding site [1]. However, the compound concomitantly activates TRPV1 receptors [4], which is undesirable for a lead structure as unwanted side effects might possibly occur. A large series of semisynthetic and fully synthetic piperine analogs was therefore synthesized, with the objective to obtain compounds with improved GABA<sub>A</sub> receptor activity and reduced TRPV1 receptor interaction [2,7,9]. Among these, the analogs SCT-66, SCT-64, SCT-29, LAU397, and LAU399 (Fig. 1) modulated GABA<sub>A</sub> receptors more potently and/or efficiently than piperine, while being devoid of TRPV1 interaction [1,2,7,9].

Drugs acting on the CNS such as GABA<sub>A</sub> receptor modulators need to penetrate the brain by crossing the BBB in order to reach their target sites. In this study, we aimed thus at early screening piperine and five promising analogs (SCT-66, SCT-64, SCT-29, LAU397, and LAU399; Fig. 1) for their ability to cross the BBB, in order to evaluate their potential as lead structures for the development of new GABA<sub>A</sub> receptor modulating drugs, and to select the most promising candidate molecule for further *in vivo* testing or for the next cycle of medicinal chemistry optimization.

The immortalized *in vitro* human BBB model based on the hBMEC cell line was recently established in our laboratory [14,15]. This cell line, which was initially generated by Stins et al. (2001) [13], was considered as the most suitable and promising cell line in terms of barrier tightness in an in-house screening of four currently available immortalized human brain capillary endothelial cell lines (hCMEC/D3, hBMEC, TY10, and BB19) [14]. Culture conditions (such as growth medium composition, 24-well tissue culture insert material, coating material and procedure, cell seeding density) were systematically optimized for hBMEC cell line [14], and TEER values were recorded by an automated CellZscope system in order to obtain highly standardized data [33]. The model was validated with a representative series of control drug substances by means of reliable UHPLC-MS/MS quantification assays [15]. TEER values for hBMEC monolayers (20–40  $\Omega\text{cm}^2$ ) [14,15] were not significantly improved when compared to TEER values reported for other *in vitro* BBB models using immortalized human cells (TEER up to 200  $\Omega\text{cm}^2$ ) [13,34,35] or primary animal cells (TEER up to 1500  $\Omega\text{cm}^2$ ) [36–39]. However, mean  $P_e$  values for the paracellular flux marker Na-F across hBMEC monolayers were in a similar range as those observed in primary animal *in vitro* BBB models (0.5–6  $\times 10^{-6}$  cm/s) [36,37].

For comparative purposes, we initially decided to select three human BBB models including immortalized, primary, and stem cell-derived human cell phenotypes. However, getting access to post-mortem human brains was critical, and we therefore utilized a highly tight animal BBB model. The compounds were thus screened in our recently established immortalized human mono-culture *in vitro* BBB model based on hBMEC cell line [13–15], in a recently developed *in vitro* human BLEC BBB model [16], and in a well-established tight primary

animal (bovine endothelial/rat astrocytes co-culture) *in vitro* BBB model [17]. For each compound, a specific quantitative UHPLC-MS/MS assay in the corresponding matrix was developed, and permeability coefficients across the endothelial monolayers were determined. For each model, we reported the permeability coefficients that are usually calculated for screened compounds (i.e.  $P_e$  for the two human models [15,16], and  $P_{app}$  for the animal model [17]).

During UHPLC-MS/MS method development, non-specific adsorption of the compounds in RHB to various surfaces was observed, leading to unacceptable calibration curves (data not shown). This problem was resolved by spiking RHB with 0.2% Tween 20 for the preparation of calibrators and QCs [40], and valid calibration curves could be obtained (Table S2). For compounds in modified DMEM, the addition of Tween 20 was only necessary for SCT-66, SCT-64, and SCT-29. For the other analogs, the presence of FBS (10%) in the matrix (DMEM) seemed to be sufficient to avoid non-specific adsorption to surfaces. However, the permeability assays could not be carried out using RHB or DMEM spiked with Tween 20 since the detergent could affect the integrity of the endothelial barrier. Thus, samples were diluted after the assays with an equal volume of the corresponding matrix containing 0.4% Tween 20 directly in the tubes for optimal desorption.

In the two human *in vitro* BBB models, piperine and SCT-64 displayed moderate to high BBB permeability, while SCT-29 and LAU397 displayed low BBB permeability (Fig. 2A and 2B, Tables 1 and 2). The analog SCT-66 showed moderate BBB permeability in the human BLEC BBB model (but low permeability in the immortalized model), while LAU399 showed moderate BBB permeation in the immortalized model (but low permeability in the human BLEC model) (Fig. 2A and 2B, Tables 1 and 2). With the exception of this minor difference, both human models provided a similar ranking of the compounds based on their  $P_{e(A\rightarrow B)}$  values.

Results from the primary animal *in vitro* BBB model were not in complete agreement with permeability data from the two human models. In the animal model, all compounds showed high BBB permeability, while in the human models, two analogs (SCT-29 and LAU397) showed low BBB permeation (Fig. 2, Tables 1–3). These data discrepancies were most likely due to the different matrices used for the permeability screenings. In the animal model, transport experiments were carried out directly in cell culture medium (i.e. DMEM containing 10% FBS). The presence of proteins in the receiver compartment thus created an additional sink, possibly increasing the permeability of the lipophilic piperine analogs across the BBB due to protein binding [41].

According to several calculated descriptor values relevant for BBB permeation (i.e. PSA, MW, H-bond acceptors and donors, and LogBB; Table 4), all compounds should be able to permeate the BBB by passive diffusion. However, a closer consideration of the descriptors LogP and number of rotatable bonds may provide an explanation for the low permeability observed for SCT-29 and LAU397 in the human BBB models. According to Brito-Sánchez et al. (2015), the total number of rotatable bonds should not exceed 6 to facilitate the permeation of a compound across the BBB [32]. For SCT-29 and LAU397, the total number of rotatable bonds of the compounds was rather high (9 and 10, respectively; counting according to Veber rules; Table 4). Furthermore, SCT-29 and LAU397 showed relatively high LogP values (4.70 and 5.34, respectively; Table 4) which are above the recommended range of 1–4 for CNS drugs. Compounds SCT-66 and SCT-64 also showed

relatively high LogP values (4.59 and 3.96, respectively). However, their total number of rotatable bonds was lower (7). In case of LAU399, the high number of rotatable bonds (9) and non-optimal lipophilicity (LogP of 5.21) were probably compensated by its extremely small PSA (26.9 Å<sup>2</sup>). Piperine showed moderate lipophilicity (LogP of 3.27), a low number of rotatable bonds (3), and was thus best suited for BBB permeation. In conclusion, it seemed that for the human models, BBB permeation of this series of compounds depended mainly on their number of rotatable bonds.

*In silico* LogBB values (logarithm of total brain-to-plasma ratio) were between -0.51 and -0.12 for all compounds (Table 4). These values seemed not to correlate well with the  $P_e$  values observed in the two human models (Tables 1 and 2). However, LogBB values are a measure of the extent of brain penetration (i.e. of the distribution of a drug between plasma and brain, which is influenced by multiple factors, such as plasma protein and brain tissue binding), while  $P_e$  values predict the rate of brain penetration (i.e. of BBB permeability by passive diffusion, active uptake, and/or efflux) [42,43]. The two parameters thus describe different aspects of brain drug penetration and are not necessarily in agreement [43,44].

In the animal *in vitro* BBB model, mean  $P_{app(A\rightarrow B)}$  values for Na-F in presence of the compounds were up to five times higher than those normally observed in this model (below  $1 \times 10^{-6}$  cm/s). However, mean  $P_{app}$  values in the direction B→A for Na-F in presence of the compounds were in this expected range (below  $1 \times 10^{-6}$  cm/s; Table S9). Thus, a polarized opening of the paracellular space may have occurred when the compounds were applied on the apical side (but not on the basolateral side). Therefore, mean  $P_{app}$  values in the direction B→A for the compounds may give a better estimation of their BBB permeability in a situation where there is no barrier opening.

For piperine, the polarized junctional effect was further investigated by separately applying the compound on the apical and basolateral side of the inserts (5 μM), and measuring the TEER as a function of incubation time. Throughout an incubation period of two hours, the TEER was relatively stable for control cell monolayers and for cell monolayers to which piperine was applied on the basolateral side (Fig. 3). However, TEER values decreased from 1261 to 268 Ωcm<sup>2</sup> for cell monolayers to which piperine was added on the apical side (Fig. 3), supporting the hypothesis of a polarized paracellular opening. The apparent junctional opening could be caused by TRPV1 activation in brain endothelial cells, as has previously been demonstrated in anesthetized rats [45]. TRPV1 activation has been shown to decrease TEER and to cause occludin redistribution in a rat submandibular gland cell line (SMG-C6) [46], and may have caused similar effects in the bovine endothelial cells, which would imply an apical localization of TRPV1 receptors in the endothelial cells. The five tested piperine analogs were reported not to act on rat TRPV1 receptors [2,9], but affinities for the bovine form of the receptor may differ. However, more detailed studies to clarify these issues would be necessary. An opening of the barrier could not be observed in the human models with compounds at 2 μM, as  $P_e$  values for Na-F in both directions ( $P_{e(A\rightarrow B)}$  see Tables 1 and 2;  $P_{e(B\rightarrow A)}$  data not shown) were in a similar range as usually obtained in the two models, indicating that barrier integrity was maintained throughout the experiments.

In previous studies, piperine and the analogs SCT-66, SCT-64, and SCT-29 were reported to exhibit anxiolytic effects in mice [2,7]. However, SCT-66 and SCT-29 did not cross the BBB significantly in the *in vitro* human models, while crossing the BBB in the *in vitro* bovine/rat model. As discussed above, the high permeability of the compounds in the animal model was likely due to the presence of FBS in the transport matrix, which created sink conditions in the receiver compartment, and thus improved  $P_{app}$  values due to protein binding of the compounds. To evaluate whether the compounds are able to reach the brain, further studies (such as protein binding, PK, and drug metabolism studies) are therefore necessary.

Finally, by performing bidirectional permeability experiments, we did not evidence any effect of active efflux transporters on compound permeation across the BBB (ER below 2; Tables S7–S9). However, piperine has been reported to inhibit P-glycoprotein (P-gp) and phase I and II metabolism enzymes [47–49]. Thus, possible inhibition of P-gp and CYPs by the compounds needs to be assessed. Also, an evaluation of the metabolic stability is needed, especially for compounds containing the metabolically critical 1,3-benzodioxole group (piperine, SCT-66, SCT-64, and SCT-29; Fig. 1).

## 5 Conclusions

Piperine and five selected piperine analogs with positive GABA<sub>A</sub> receptor modulatory activity were screened in three *in vitro* cell-based human and animal BBB models for their ability to cross the BBB. Data from the three models differed to some extent, possibly due to protein binding of the piperine analogs. In all three models, piperine and SCT-64 displayed the highest BBB permeation potential, which could be corroborated by *in silico* prediction data. For the other piperine analogs (SCT-66, SCT-29, LAU397, and LAU399), BBB permeability was low to moderate in the two human models, and moderate to high in the animal model. ER calculated from bidirectional permeability experiments indicated that the compounds were likely not substrates of active efflux. In addition to the early *in vitro* BBB permeability assessment of the compounds, further studies (such as PK and drug metabolism studies) are currently in progress in our laboratory. Taken together, these data will serve for selecting the most promising candidate molecule for the next cycle of medicinal chemistry optimization.

## Acknowledgments

The authors are grateful to Prof. Kwang Sik Kim, Prof. Dennis Grab, Prof. Reto Brun, and Dr. Tanja Wenzler for providing the hBMEC cell line. Further thanks go to Orlando Fertig for technical assistance, and to Tabea Gollin for contribution to the graphical abstract. Hans Christian Cederberg Helms and Birger Brodin acknowledge the support from the Lundbeck Foundation via the “Research Initiative on Brain Barriers and Drug Delivery” (RIBBDD) grant. Laurin Wimmer is a fellow of the doctoral program W-1232 of the Austrian Research Fund (FWF). This research was supported by the Swiss National Science Foundation (SNSF) (grant 05320\_126888/1 to MH).

## Conflict of interest

The authors declare no conflict of interest.

## References

- [1] J. Zaugg, I. Baburin, B. Strommer, H.-J. Kim, S. Hering, M. Hamburger, HPLC-based activity profiling: discovery of piperine as a positive GABAA receptor modulator targeting a benzodiazepine-independent binding site, *J. Nat. Prod.* 73 (2010) 185–191.
- [2] S. Khom, B. Strommer, A. Schöffmann, J. Hintersteiner, I. Baburin, T. Erker, et al., GABAA receptor modulation by piperine and a non-TRPV1 activating derivative, *Biochem. Pharmacol.* 85 (2013) 1827–1836.
- [3] H. Möhler, GABAA receptors in central nervous system disease: anxiety, epilepsy, and insomnia, *J. Recept. Signal Transduct.* 26 (2006) 731–740.
- [4] F.N. McNamara, A. Randall, M.J. Gunthorpe, Effects of piperine, the pungent component of black pepper, at the human vanilloid receptor (TRPV1), *Br. J. Pharmacol.* 144 (2005) 781–790.
- [5] V. Di Marzo, G. Gobbi, A. Szallasi, Brain TRPV1: a depressing TR(i)P down memory lane?, *Trends Pharmacol. Sci.* 29 (2008) 594–600.
- [6] N.R. Gavva, A.W. Bannon, S. Surapaneni, D.N. Hovland, S.G. Lehto, A. Gore, et al., The vanilloid receptor TRPV1 is tonically activated in vivo and involved in body temperature regulation, *J. Neurosci.* 27 (2007) 3366–3374.
- [7] A. Schöffmann, L. Wimmer, D. Goldmann, S. Khom, J. Hintersteiner, I. Baburin, et al., Efficient modulation of  $\gamma$ -aminobutyric acid type A receptors by piperine derivatives, *J. Med. Chem.* 57 (2014) 5602–5619.
- [8] S.M. Attia, Deleterious effects of reactive metabolites, *Oxid. Med. Cell. Longev.* 3 (2010) 238–253.
- [9] L. Wimmer, D. Schönbauer, P. Pakfeifer, A. Schöffmann, S. Khom, S. Hering, et al., Developing piperine towards TRPV1 and GABAA receptor ligands – synthesis of piperine analogs via Heck-coupling of conjugated dienes, *Org. Biomol. Chem.* 13 (2015) 990–994.
- [10] N.J. Abbott, A.A.K. Patabendige, D.E.M. Dolman, S.R. Yusof, D.J. Begley, Structure and function of the blood-brain barrier, *Neurobiol. Dis.* 37 (2010) 13–25.
- [11] L. Di, H. Rong, B. Feng, Demystifying brain penetration in central nervous system drug discovery, *J. Med. Chem.* 56 (2013) 2–12.
- [12] A. Reichel, Addressing central nervous system (CNS) penetration in drug discovery: basics and implications of the evolving new concept, *Chem. Biodivers.* 6 (2009) 2030–2049.
- [13] M.F. Stins, J. Badger, K.S. Kim, Bacterial invasion and transcytosis in transfected human brain microvascular endothelial cells, *Microb. Pathog.* 30 (2001) 19–28.
- [14] D.E. Eigenmann, G. Xue, K.S. Kim, A.V. Moses, M. Hamburger, M. Oufir, Comparative study of four immortalized human brain capillary endothelial cell lines, hCMEC/D3, hBMEC, TY10, and BB19, and optimization of culture conditions, for an in vitro blood-brain barrier model for drug permeability studies, *Fluids Barriers CNS.* 10 (2013) 33–50.
- [15] D.E. Eigenmann, E.A. Jähne, M. Smieško, M. Hamburger, M. Oufir, Validation of an immortalized human (hBMEC) in vitro blood-brain barrier model, *Anal. Bioanal. Chem.* 408 (2016) 2095–2107.
- [16] R. Cecchelli, S. Aday, E. Sevin, C. Almeida, M. Culot, L. Dehouck, et al., A stable and reproducible human blood-brain barrier model derived from hematopoietic stem cells, *PLoS ONE.* 9 (2014) 1–11.
- [17] H.C. Helms, B. Brodin, Generation of primary cultures of bovine brain endothelial cells and setup of cocultures with rat astrocytes, in: R. Milner (Ed.), *Cereb. Angiogenesis*, Springer New York, 2014: pp. 365–382.
- [18] Guidance for Industry: Bioanalytical Method Validation, US Food and Drug Administration (FDA), Center for Drug Evaluation and Research (CDER), May 2001, (n.d.).
- [19] Guideline on bioanalytical method validation, European Medicines Agency (EMA/CHMP/EWP/192217/2009), London, 21 July 2011, (n.d.).
- [20] A. Siflinger-Birnboim, P.J. del Vecchio, J.A. Cooper, F.A. Blumenstock, J.M. Shepard, A.B. Malik, Molecular sieving characteristics of the cultured endothelial monolayer, *J. Cell. Physiol.* 132 (1987) 111–117.
- [21] M.-P. Dehouck, P. Jolliet-Riant, F. Brée, J.-C. Fruchart, R. Cecchelli, J.-P. Tillement, Drug transfer across the blood-brain barrier: correlation between in vitro and in vivo models, *J. Neurochem.* 58 (1992) 1790–1797.
- [22] S. Lundquist, M. Renftel, J. Brillault, L. Fenart, R. Cecchelli, M.-P. Dehouck, Prediction of drug transport through the blood-brain barrier in vivo: a comparison between two in vitro cell models, *Pharm. Res.* 19 (2002) 976–981.
- [23] E. Hellinger, S. Veszelka, A.E. Toth, F. Walter, A. Kittel, M.L. Bakk, et al., Comparison of brain capillary endothelial cell-based and epithelial (MDCK-MDR1, Caco-2, and VB-Caco-2) cell-based surrogate blood-brain barrier penetration models, *Eur. J. Pharm. Biopharm.* 82 (2012) 340–351.

- [24] J.W. Polli, S.A. Wring, J.E. Humphreys, L. Huang, J.B. Morgan, L.O. Webster, et al., Rational use of in vitro P-glycoprotein assays in drug discovery, *J. Pharmacol. Exp. Ther.* 299 (2001) 620–628.
- [25] K.M. Giacomini, S.-M. Huang, D.J. Tweedie, L.Z. Benet, K.L.R. Brouwer, X. Chu, et al., Membrane transporters in drug development, *Nat. Rev. Drug Discov.* 9 (2010) 215–236.
- [26] Maestro, version 9.9, Schrödinger, LLC, New York, NY, 2014, (n.d.).
- [27] QikProp, version 4.1, Schrödinger, LLC, New York, NY, 2014, (n.d.).
- [28] Marvin 15.4.13.0, 2015, ChemAxon (<http://www.chemaxon.com>), (n.d.).
- [29] C.A. Bertrand, D.M. Durand, G.M. Saidel, C. Laboisse, U. Hopfer, System for dynamic measurements of membrane capacitance in intact epithelial monolayers, *Biophys. J.* 75 (1998) 2743–2756.
- [30] J. Kelder, P.D. Grootenhuys, D.M. Bayada, L.P. Delbressine, J.P. Ploemen, Polar molecular surface as a dominating determinant for oral absorption and brain penetration of drugs, *Pharm. Res.* 16 (1999) 1514–1519.
- [31] H. van de Waterbeemd, G. Camenisch, G. Folkers, J.R. Chretien, O.A. Raevsky, Estimation of blood-brain barrier crossing of drugs using molecular size and shape, and H-bonding descriptors, *J. Drug Target.* 6 (1998) 151–165.
- [32] Y. Brito-Sánchez, Y. Marrero-Ponce, S.J. Barigye, I. Yaber-Goenaga, C. Morell Pérez, H. Le-Thi-Thu, et al., Towards better BBB passage prediction using an extensive and curated data set, *Mol. Inform.* 34 (2015) 308–330.
- [33] J. Wegener, D. Abrams, W. Willenbrink, H.-J. Galla, A. Janshoff, Automated multi-well device to measure transepithelial electrical resistances under physiological conditions, *BioTechniques.* 37 (2004) 590–597.
- [34] B.B. Weksler, E.A. Subileau, N. Perriere, P. Charneau, K. Holloway, M. Leveque, et al., Blood-brain barrier-specific properties of a human adult brain endothelial cell line, *FASEB J.* 19 (2005) 1872–1874.
- [35] T. Maeda, Y. Sano, M. Abe, F. Shimizu, Y. Kashiwamura, S. Ohtsuki, et al., Establishment and characterization of spinal cord microvascular endothelial cell lines, *Clin. Exp. Neuroimmunol.* 4 (2013) 326–338.
- [36] S. Nakagawa, M.A. Deli, H. Kawaguchi, T. Shimizudani, T. Shimono, A. Kittel, et al., A new blood-brain barrier model using primary rat brain endothelial cells, pericytes and astrocytes, *Neurochem. Int.* 54 (2009) 253–263.
- [37] H.C. Helms, H.S. Waagepetersen, C.U. Nielsen, B. Brodin, Paracellular tightness and claudin-5 expression is increased in the BCEC/astrocyte blood-brain barrier model by increasing media buffer capacity during growth, *AAPS J.* 12 (2010) 759–770.
- [38] A. Patabendige, R.A. Skinner, N.J. Abbott, Establishment of a simplified in vitro porcine blood-brain barrier model with high transendothelial electrical resistance, *Brain Res.* 1521 (2012) 1–15.
- [39] M.-P. Dehouck, S. Meresse, P. Delorme, J.-C. Fruchart, R. Cecchelli, An easier, reproducible, and mass-production method to study the blood-brain barrier in vitro, *J. Neurochem.* 54 (1990) 1798–1801.
- [40] A.J. Ji, Z. Jiang, Y. Livson, J.A. Davis, J.X. Chu, N. Weng, Challenges in urine bioanalytical assays: overcoming nonspecific binding, *Bioanalysis.* 2 (2010) 1573–1586.
- [41] I. Hubatsch, E.G.E. Ragnarsson, P. Artursson, Determination of drug permeability and prediction of drug absorption in Caco-2 monolayers, *Nat. Protoc.* 2 (2007) 2111–2119.
- [42] Z. Rankovic, CNS drug design: balancing physicochemical properties for optimal brain exposure, *J. Med. Chem.* 58 (2015) 2584–2608.
- [43] M. Hammarlund-Udenaes, M. Fridén, S. Syvänen, A. Gupta, On the rate and extent of drug delivery to the brain, *Pharm. Res.* 25 (2008) 1737–1750.
- [44] M. Hammarlund-Udenaes, The use of microdialysis in CNS drug delivery studies: Pharmacokinetic perspectives and results with analgesics and antiepileptics, *Adv. Drug Deliv. Rev.* 45 (2000) 283–294.
- [45] D.-E. Hu, A.S. Easton, P.A. Fraser, TRPV1 activation results in disruption of the blood-brain barrier in the rat, *Br. J. Pharmacol.* 146 (2005) 576–584.
- [46] X. Cong, Y. Zhang, N.-Y. Yang, J. Li, C. Ding, Q.-W. Ding, et al., Occludin is required for TRPV1-modulated paracellular permeability in the submandibular gland, *J. Cell Sci.* 126 (2013) 1109–1121.
- [47] R.K. Bhardwaj, H. Glaeser, L. Becquemont, U. Klotz, S.K. Gupta, M.F. Fromm, Piperine, a major constituent of black pepper, inhibits human P-glycoprotein and CYP3A4, *J. Pharmacol. Exp. Ther.* 302 (2002) 645–650.
- [48] Y. Han, T.M. Chin Tan, L.-Y. Lim, In vitro and in vivo evaluation of the effects of piperine on P-gp function and expression, *Toxicol. Appl. Pharmacol.* 230 (2008) 283–289.
- [49] L.P. Volak, S. Ghirmai, J.R. Cashman, M.H. Court, Curcuminoids inhibit multiple human cytochromes P450, UDP-glucuronosyltransferase, and sulfotransferase enzymes, whereas piperine is a relatively selective CYP3A4 inhibitor, *Drug Metab. Dispos.* 36 (2008) 1594–1605.

## FIGURES

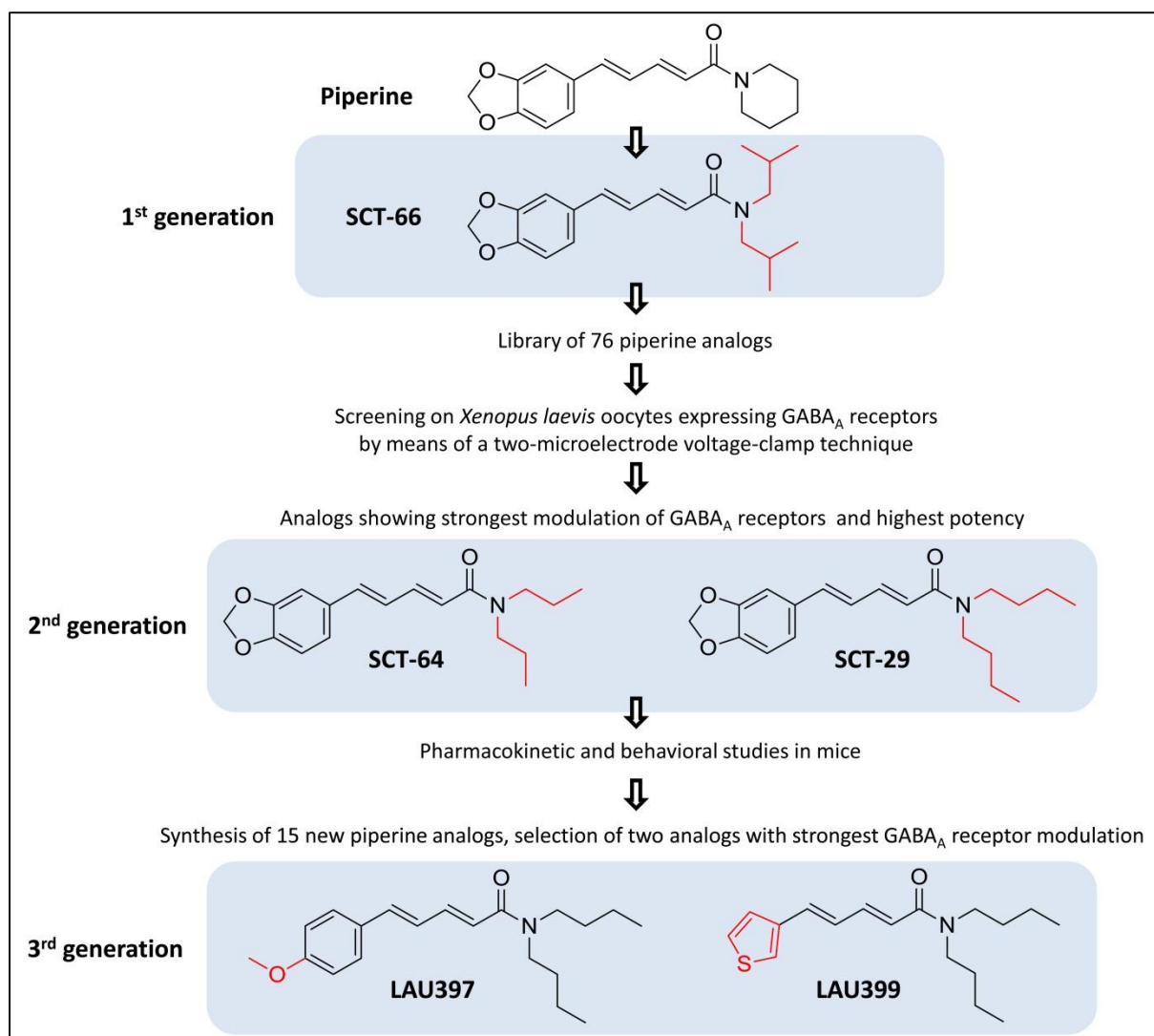


**Fig. 1** Piperine and analogs analyzed in the *in vitro* BBB models. Selection and optimization process, and structures of compounds [1,2,7,9].

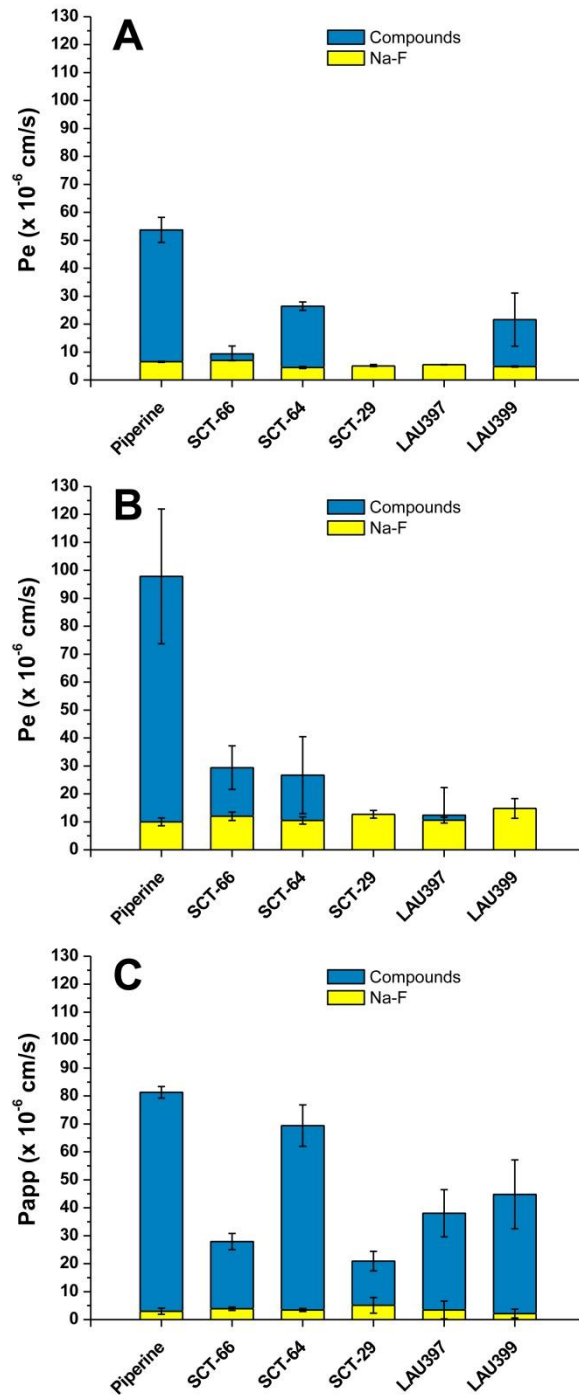


**Fig. 2** Mean endothelial permeability coefficients ( $P_{e(A \rightarrow B)} \pm SD$ ) for piperine and five analogs in (A) the immortalized *in vitro* human BBB model (hBMEC cell line-based), (B) the *in vitro* human BLEC BBB model, and (C) mean apparent permeability coefficients ( $P_{app(A \rightarrow B)} \pm SD$ ) in the *in vitro* primary bovine endothelial/rat astrocytes co-culture BBB model.

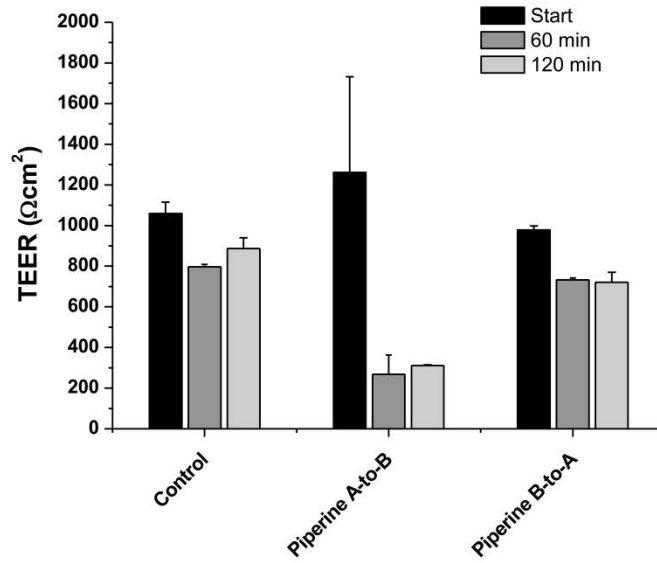


**Fig. 3** Mean TEER  $\pm$  SD values in the primary bovine endothelial/rat astrocytes co-culture *in vitro* BBB model for endothelial cell monolayers as a function of incubation time ( $n = 2$ ). TEER values were relatively stable for a two hour incubation time for control cell monolayers, and for cell monolayers when piperine ( $5 \mu\text{M}$ ) was applied on the basolateral side (Piperine B-to-A). However, TEER values of cell monolayers decreased from 1261 to 268  $\Omega\text{cm}^2$  when piperine ( $5 \mu\text{M}$ ) was applied on the apical side (Piperine A-to-B), suggesting a polarized opening of the paracellular space.

## **TABLES**

**Table 1** Mean endothelial permeability coefficients ( $P_{e(A \rightarrow B)}$ ) for analytes and Na-F, and mean recoveries for analytes obtained in the immortalized *in vitro* human BBB model based on hBMEC cell line (n = 3–4).

<b>Compound</b>	<b>Mean <math>P_e \pm SD</math> (x <math>10^{-6}</math> cm/s)</b>	<b>Na-F: Mean <math>P_e \pm SD</math> (x <math>10^{-6}</math> cm/s)</b>	<b>Mean recovery <math>\pm SD</math> for analyte (%)*</b>
<b>Direction</b>	<b>A <math>\rightarrow</math> B</b>	<b>A <math>\rightarrow</math> B</b>	<b>A <math>\rightarrow</math> B</b>
Piperine	53.7 $\pm$ 4.47	6.51 $\pm$ 0.163	107 $\pm$ 5.59
SCT-66	9.32 $\pm$ 2.82	7.01 $\pm$ 0.0817	86.7 $\pm$ 15.3
SCT-64	26.4 $\pm$ 1.48	4.50 $\pm$ 0.387	70.4 $\pm$ 4.55
SCT-29	4.29 $\pm$ 1.25	4.99 $\pm$ 0.205	88.2 $\pm$ 8.73
LAU397	4.49 $\pm$ 1.07	5.45 $\pm$ 0.0609	88.2 $\pm$ 3.41
LAU399	21.6 $\pm$ 9.52	4.83 $\pm$ 0.188	97.5 $\pm$ 13.3

\*Recoveries were assessed with the experimental concentrations of the working solutions.

**Table 2** Mean endothelial permeability coefficients ( $P_{e(A \rightarrow B)}$ ) for analytes and Na-F, and mean recoveries for analytes obtained in the *in vitro* human BLEC BBB model (n = 3).

<b>Compound</b>	<b>Mean <math>P_e \pm SD</math> (x <math>10^{-6}</math> cm/s)</b>	<b>Na-F: Mean <math>P_e \pm SD</math> (x <math>10^{-6}</math> cm/s)</b>	<b>Mean recovery <math>\pm SD</math> for analyte (%)*</b>
<b>Direction</b>	<b>A <math>\rightarrow</math> B</b>	<b>A <math>\rightarrow</math> B</b>	<b>A <math>\rightarrow</math> B</b>
Piperine	97.8 $\pm$ 24.1	9.99 $\pm$ 1.41	97.0 $\pm$ 8.02
SCT-66	29.4 $\pm$ 7.79	12.0 $\pm$ 1.47	68.5 $\pm$ 9.49
SCT-64	26.7 $\pm$ 13.8	10.5 $\pm$ 1.32	61.2 $\pm$ 5.83
SCT-29	4.61 $\pm$ 1.29	12.7 $\pm$ 1.38	56.1 $\pm$ 10.4
LAU397	12.4 $\pm$ 9.91	10.6 $\pm$ 1.05	55.7 $\pm$ 2.54
LAU399	7.79 $\pm$ 2.64	14.8 $\pm$ 3.57	60.1 $\pm$ 1.55

\*Recoveries were assessed with the experimental concentrations of the working solutions.

**Table 3** Mean apparent permeability coefficients ( $P_{app(A \rightarrow B)}$ ) for analytes and Na-F, and mean recoveries for analytes obtained in the primary bovine endothelial/rat astrocytes co-culture *in vitro* BBB model (n = 3).

<b>Compound</b>	<b>Mean <math>P_{app} \pm SD</math> (x <math>10^{-6}</math> cm/s)</b>	<b>Na-F: Mean <math>P_{app} \pm SD</math> (x <math>10^{-6}</math> cm/s)</b>	<b>Mean recovery <math>\pm SD</math> for analyte (%)*</b>
<b>Direction</b>	<b>A <math>\rightarrow</math> B</b>	<b>A <math>\rightarrow</math> B</b>	<b>A <math>\rightarrow</math> B</b>
Piperine	81.3 $\pm$ 2.04	3.00 $\pm$ 1.12	120 $\pm$ 5.70
SCT-66	27.9 $\pm$ 2.90	3.88 $\pm$ 0.573	78.4 $\pm$ 6.50
SCT-64	69.4 $\pm$ 7.40	3.39 $\pm$ 0.530	96.6 $\pm$ 3.20
SCT-29	20.9 $\pm$ 3.48	5.07 $\pm$ 2.81	68.4 $\pm$ 2.80
LAU397	38.0 $\pm$ 8.44	3.42 $\pm$ 3.19	125 $\pm$ 9.70
LAU399	44.8 $\pm$ 12.3	2.15 $\pm$ 1.58	118 $\pm$ 3.70

\*Recoveries were assessed with the experimental concentrations of the working solutions.

**Table 4** *In silico* calculation of BBB permeation for piperine and analogs.

Compounds	QikProp descriptors (3D based)							Marvin descriptors		Rotatable bonds <sup>f</sup>		
	MW	donorHB <sup>a</sup>	acceptHB <sup>b</sup>	PSA (Å <sup>2</sup> )	LogP (o/w)	Human Oral Absorption (%)	LogBB <sup>c</sup>	QPPCaco <sup>d</sup> (nm/s)	QPPMDCK <sup>e</sup> (nm/s)		PSA (Å <sup>2</sup> )	LogP
Piperine	285.3	0	4.5	48.1	3.27	100	-0.12	3996	2211	38.8	2.78	3
SCT-66	329.4	0	4.5	43.6	4.59	100	-0.25	5441	3087	38.8	4.42	7
SCT-64	301.4	0	4.5	45.5	3.96	100	-0.29	4893	2753	38.8	3.69	7
SCT-29	329.4	0	4.5	45.3	4.70	100	-0.42	4923	2772	38.8	4.57	9
LAU397	315.5	0	3.75	35.1	5.34	100	-0.51	4869	2739	29.5	4.79	10
LAU399	291.5	0	3	26.9	5.21	100	-0.30	4877	5545	20.3	4.72	9

<sup>a</sup>donorHB: donor hydrogen bonds; <sup>b</sup>acceptHB: acceptor hydrogen bonds; <sup>c</sup>LogBB: Predicted brain/blood partition coefficient (for 95% of known drugs, values range between -3.0 and 1.2); <sup>d</sup>QPPCaco: predicted apparent Caco-2 cell permeability in nm/s (< 25 poor, > 500 great); <sup>e</sup>QPPMDCK: predicted apparent Madin-Darby Canine Kidney (MDCK) cell permeability in nm/s (< 25 poor, > 500 great); <sup>f</sup>Counting according to Veber rules.

## **ELECTRONIC SUPPLEMENTARY MATERIAL**

### ***In vitro* blood-brain barrier permeability predictions for GABA<sub>A</sub> receptor modulating piperine analogs**

Daniela Elisabeth Eigenmann<sup>a</sup>, Carmen Dürig<sup>a</sup>, Evelyn Andrea Jähne<sup>a</sup>, Martin Smieško<sup>b</sup>, Maxime Culot<sup>c</sup>, Fabien Gosselet<sup>c</sup>, Romeo Cecchelli<sup>c</sup>, Hans Christian Cederberg Helms<sup>d</sup>, Birger Brodin<sup>d</sup>, Laurin Wimmer<sup>e</sup>, Marko D. Mihovilovic<sup>e</sup>, Matthias Hamburger<sup>a</sup>, and Mouhssin Oufir<sup>a,\*</sup>

<sup>a</sup>Pharmaceutical Biology, Department of Pharmaceutical Sciences, University of Basel, Klingelbergstrasse 50, CH-4056 Basel, Switzerland

<sup>b</sup>Molecular Modeling, Department of Pharmaceutical Sciences, University of Basel, Klingelbergstrasse 50, CH-4056 Basel, Switzerland

<sup>c</sup>Univ. Artois, EA 2465, Laboratoire de la Barrière Hémato-Encéphalique (LBHE), F-62300 Lens Cedex, France

<sup>d</sup>Drug Transporters in ADME, Department of Pharmacy, Faculty of Health and Medical Sciences, University of Copenhagen, Universitetsparken 2, DK-2100 Copenhagen, Denmark

<sup>e</sup>Institute of Applied Synthetic Chemistry, TU Wien, Getreidemarkt 9, A-1060 Vienna, Austria

\*Corresponding author. Pharmaceutical Biology, Department of Pharmaceutical Sciences, University of Basel, Klingelbergstrasse 50, CH-4056 Basel, Switzerland. Tel: +41 61 2671425; fax: +41 61 2671474.

E-mail address: mouhssin.oufir@unibas.ch (M. Oufir).

## FIGURES

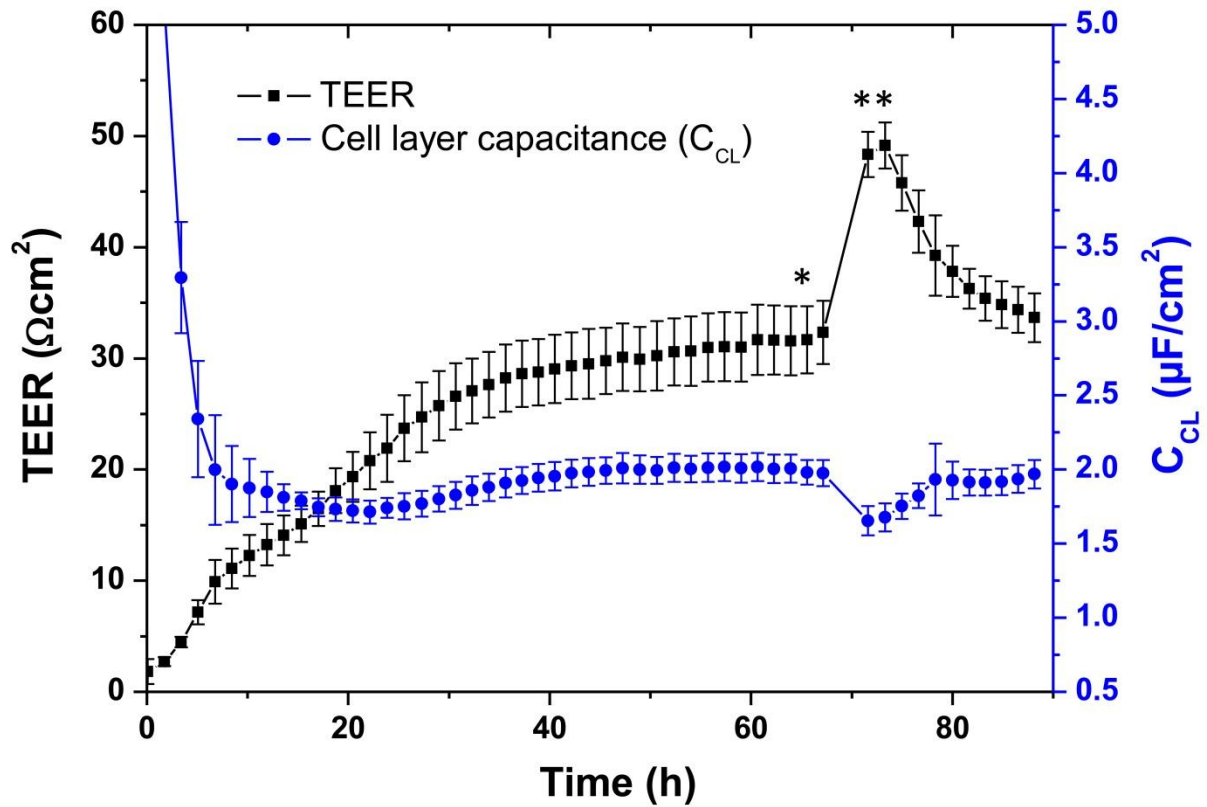


**Fig. S1** Mean TEER  $\pm$  SD values (black curve) and mean cell layer capacitance ( $C_{CL}$ )  $\pm$  SD values (blue curve) recorded in real-time by the CellZscope system of hBMEC cell monolayers grown on 24-well tissue culture inserts ( $n = 14$ ).  $C_{CL}$  values in the range of 0.5–5.0  $\mu\text{F}/\text{cm}^2$  indicate cell confluency and validate TEER values. \*Permeability assay with SCT-64. \*\*CellZscope transferred back into incubator (37°C, 5%  $\text{CO}_2$ ) for barrier integrity control.

**TABLES****Table S1** Optimized MS/MS parameters (MRM transitions, fragmentor voltage, and collision energy) in ESI+ mode for analytes and corresponding I.S.

<b>Analyte I.S.</b>	<b>MRM transitions</b>	<b>Fragmentor voltage (V)</b>	<b>Collision energy (V)</b>
Piperine (Quantifier)	286.15 → 115.00	117	54
Piperine (Qualifier)	286.15 → 143.00	117	34
I.S. SCT-64	302.18 → 115.00	117	58
SCT-66 (Quantifier)	330.21 → 201.10	127	22
SCT-66 (Qualifier)	330.21 → 115.10	127	62
I.S. SCT-64	302.18 → 115.00	117	58
SCT-64 (Quantifier)	302.18 → 115.00	117	58
SCT-64 (Qualifier)	302.18 → 143.00	117	34
I.S. SCT-66	330.21 → 201.10	127	22
SCT-29 (Quantifier)	330.21 → 201.00	177	22
SCT-29 (Qualifier)	330.21 → 115.00	177	62
I.S. SCT-64	302.18 → 115.00	117	58
LAU397 (Quantifier)	316.23 → 187.00	205	18
LAU397 (Qualifier)	316.23 → 144.00	205	38
I.S. LAU399	292.18 → 163.00	205	18
LAU399 (Quantifier)	292.18 → 163.00	205	18
LAU399 (Qualifier)	292.18 → 91.10	205	54
I.S. SCT-64	302.18 → 115.00	117	58

**Table S2** Calibrators and calibration curve parameters for analytes in modified RHB. Response:  $A \times \text{Conc.}^2 + B \times \text{Conc.} + C$ , quadratic regression, weighting factor  $1/X$ , origin: included (n = 4–6).

Compounds		Nominal concentration (ng/mL)							Regression parameters			
		5.00	25.0	50.0	100	200	400	500	A	B	C	R <sup>2</sup>
<b>Piperine</b>	Mean	5.03	24.8	49.9	99.7	204	392	507	-0.0000429	0.141	-0.00451	0.9970
	S.D.	0.214	1.34	1.53	5.75	13.1	31.2	16.7	0.0000318	0.0228	-	-
	CV%	4.25	5.42	3.07	5.76	6.45	7.97	3.29	-	-	-	-
	RE%	0.549	-0.871	-0.140	-0.259	1.81	-2.11	1.44	-	-	-	-
<b>SCT-66</b>	Mean	4.85	25.8	48.7	99.6	199	401	500	0.000000456	0.00854	0.00587	0.9977
	S.D.	0.120	1.44	2.78	5.86	7.69	17.9	20.2	0.000000519	0.00468	-	-
	CV%	2.47	5.59	5.72	5.88	3.87	4.46	4.04	-	-	-	-
	RE%	-2.94	3.18	-2.67	-0.412	-0.457	0.162	-0.0419	-	-	-	-
<b>SCT-64</b>	Mean	4.88	25.6	51.0	97.5	197	413	493	0.000000141	0.00116	-0.000231	0.9945
	S.D.	0.424	1.84	3.60	6.88	10.4	34.7	22.0	0.000000375	0.000348	-	-
	CV%	8.69	7.17	7.05	7.06	5.29	8.40	4.46	-	-	-	-
	RE%	-2.47	2.55	2.07	-2.48	-1.60	3.17	-1.48	-	-	-	-
<b>SCT-29</b>	Mean	5.20	24.6	48.2	99.6	201	407	494	0.00000112	0.0242	-0.00513	0.9987
	S.D.	0.296	1.28	1.94	3.41	4.52	17.1	12.6	0.00000201	0.00461	-	-
	CV%	5.70	5.22	4.02	3.42	2.25	4.21	2.55	-	-	-	-
	RE%	4.06	-1.66	-3.51	-0.446	0.349	1.74	-1.11	-	-	-	-
<b>LAU397</b>	Mean	5.05	25.2	48.7	101	201	399	501	0.000000221	0.0102	0.0000172	0.9953
	S.D.	0.446	2.40	3.40	7.54	17.4	31.6	26.3	0.00000122	0.00246	-	-
	CV%	8.84	9.53	6.99	7.49	8.64	7.93	5.25	-	-	-	-
	RE%	0.961	0.617	-2.70	0.716	0.671	-0.372	0.138	-	-	-	-
<b>LAU399</b>	Mean	4.83	24.8	51.9	102	193	403	499	0.00000313	0.0127	0.000294	0.9972
	S.D.	0.0960	1.40	3.58	8.01	13.9	9.28	21.3	0.00000351	0.00166	-	-
	CV%	1.99	5.64	6.88	7.86	7.18	2.30	4.27	-	-	-	-
	RE%	-3.50	-0.701	3.89	1.96	-3.47	0.774	-0.227	-	-	-	-

**Table S3** Calibrators and calibration curve parameters for analytes in modified DMEM. Response:  $A \times \text{Conc.}^2 + B \times \text{Conc.} + C$ , quadratic regression, weighting factor  $1/X$ , origin: included (n = 4–6).

Compounds		Nominal concentration (ng/mL)							Regression parameters			
		5.00	25.0	50.0	100	200	400	500	A	B	C	R <sup>2</sup>
<b>Piperine</b>	Mean	4.81	26.1	51.3	102	195	399	503	-0.00000140	0.00329	0.00150	0.9993
	S.D.	0.250	1.78	1.09	3.73	4.80	11.4	7.42	0.000000268	0.000188	-	-
	CV%	5.20	6.81	2.13	3.68	2.46	2.87	1.48	-	-	-	-
	RE%	-3.90	4.55	2.61	1.61	-2.37	-0.247	0.600	-	-	-	-
<b>SCT-66</b>	Mean	4.94	24.8	50.0	105	198	394	506	-0.00000231	0.0132	-0.0000265	0.9982
	S.D.	0.180	0.845	3.20	9.55	9.78	9.61	10.7	0.00000164	0.00178	-	-
	CV%	3.65	3.41	6.39	9.12	4.93	2.44	2.12	-	-	-	-
	RE%	-1.21	-0.966	-0.0246	4.81	-0.794	-1.58	1.12	-	-	-	-
<b>SCT-64</b>	Mean	4.92	25.3	50.0	100	200	398	502	0.000000117	0.000971	0.000155	0.9993
	S.D.	0.250	1.03	1.60	4.57	5.32	6.62	11.3	0.000000466	0.000153	-	-
	CV%	5.08	4.08	3.20	4.54	2.66	1.66	2.24	-	-	-	-
	RE%	-1.53	1.10	-0.0164	0.481	-0.0658	-0.585	0.354	-	-	-	-
<b>SCT-29</b>	Mean	4.88	25.9	50.4	100	199	400	501	0.00000855	0.0815	0.0253	0.9990
	S.D.	0.256	0.701	1.22	3.05	3.48	14.5	15.1	0.00000607	0.0147	-	-
	CV%	5.24	2.71	2.42	3.07	1.75	3.63	3.02	-	-	-	-
	RE%	-2.34	3.41	0.778	-0.418	-0.323	-0.0902	0.108	-	-	-	-
<b>LAU397</b>	Mean	4.72	25.8	50.8	101	199	392	507	-0.000000531	0.00389	0.000852	0.9996
	S.D.	0.144	0.990	0.865	1.91	3.28	1.73	5.93	0.000000351	0.000345	-	-
	CV%	3.06	3.84	1.70	1.88	1.65	0.440	1.17	-	-	-	-
	RE%	-5.64	3.26	1.55	1.16	-0.608	-2.04	1.38	-	-	-	-
<b>LAU399</b>	Mean	5.24	24.6	48.4	103	204	390	506	0.000000955	0.00264	-0.00201	0.9988
	S.D.	0.234	3.01	2.22	3.08	4.58	8.13	7.69	0.000000116	0.000274	-	-
	CV%	4.46	12.3	4.59	2.98	2.25	2.09	1.52	-	-	-	-
	RE%	4.89	-1.70	-3.18	3.10	1.82	-2.58	1.25	-	-	-	-

**Table S4** Carry-over assessment for analytes and corresponding I.S. (n = 4–6).

<b>Compounds</b>	<b>Mean carry-over (%) in modified RHB</b>	<b>Mean carry-over (%) in modified DMEM</b>
Piperine	0.928	4.27
I.S. SCT-64	0.00	0.0501
SCT-66	0.266	1.61
I.S. SCT-64	0.00	0.0444
SCT-64	0.00	0.355
I.S. SCT-66	0.0130	0.0139
SCT-29	2.03	3.35
I.S. SCT-64	0.00	0.0140
LAU397	0.747	3.74
I.S. LAU399	0.00	0.0597
LAU399	0.00	3.70
I.S. SCT-64	0.00	0.0152

**Table S5** Between-run imprecision (CV%) and inaccuracy (RE%) of QCs in modified RHB, based on 3 series of 2 replicates for each level (n = 6).

<b>Compounds</b>		<b>Nominal concentration (ng/mL)</b>				
		<b>5.00</b>	<b>15.0</b>	<b>250</b>	<b>400</b>	<b>500</b>
<b>Piperine</b>	Mean	5.03	14.3	257	384	507
	S.D.	0.214	2.12	12.2	28.5	16.7
	CV%	4.25	14.9	4.76	7.43	3.29
	RE%	0.549	-4.97	2.81	-4.08	1.44
<b>SCT-66</b>	Mean	4.85	15.9	261	389	500
	S.D.	0.120	1.00	17.8	7.20	20.2
	CV%	2.47	6.27	6.80	1.85	4.04
	RE%	-2.94	5.76	4.52	-2.65	-0.0419
<b>SCT-64</b>	Mean	4.88	14.5	241	374	493
	S.D.	0.424	1.62	24.9	11.1	22.0
	CV%	8.69	11.2	10.3	2.98	4.46
	RE%	-2.47	-3.65	-3.59	-6.51	-1.48
<b>SCT-29</b>	Mean	5.20	16.5	244	397	494
	S.D.	0.296	1.37	22.0	36.3	12.6
	CV%	5.70	8.30	9.04	9.13	2.55
	RE%	4.06	9.98	-2.59	-0.735	-1.11
<b>LAU397</b>	Mean	5.05	15.2	256	398	501
	S.D.	0.446	0.918	11.0	7.98	26.3
	CV%	8.84	6.05	4.31	2.01	5.25
	RE%	0.961	1.25	2.54	-0.605	0.138
<b>LAU399</b>	Mean	4.83	16.0	264	403	499
	S.D.	0.0960	1.39	12.3	41.5	21.3
	CV%	1.99	8.68	4.65	10.3	4.27
	RE%	-3.50	6.81	5.63	0.851	-0.227

**Table S6** Between-run imprecision (CV%) and inaccuracy (RE%) of QCs in modified DMEM, based on 3 series of 2 replicates for each level (n = 6).

Compounds		Nominal concentration (ng/mL)				
		5.00	15.0	250	400	500
<b>Piperine</b>	Mean	4.81	15.9	247	393	503
	S.D.	0.250	1.09	22.1	8.64	7.42
	CV%	5.20	6.83	8.93	2.20	1.48
	RE%	-3.90	6.17	-1.17	-1.73	0.600
<b>SCT-66</b>	Mean	4.94	16.4	253	384	506
	S.D.	0.180	1.23	20.3	17.0	10.7
	CV%	3.65	7.54	8.05	4.42	2.12
	RE%	-1.21	9.13	1.03	-3.95	1.12
<b>SCT-64</b>	Mean	4.92	13.8	230	375	502
	S.D.	0.250	0.658	9.41	6.79	11.3
	CV%	5.08	4.75	4.10	1.81	2.24
	RE%	-1.53	-7.72	-8.15	-6.14	0.354
<b>SCT-29</b>	Mean	4.88	16.4	269	394	501
	S.D.	0.256	0.566	12.1	22.5	15.1
	CV%	5.24	3.46	4.50	5.71	3.02
	RE%	-2.34	9.11	7.77	-1.40	0.108
<b>LAU397</b>	Mean	4.72	16.5	242	379	507
	S.D.	0.144	1.22	14.8	9.78	5.93
	CV%	3.06	7.41	6.11	2.58	1.17
	RE%	-5.64	9.77	-3.35	-5.37	1.38
<b>LAU399</b>	Mean	5.24	16.5	254	408	506
	S.D.	0.234	0.431	10.1	13.7	7.69
	CV%	4.46	2.61	4.00	3.36	1.52
	RE%	4.89	10.0	1.42	1.97	1.25

**Table S7** Mean apparent permeability coefficients ( $P_{app(A\rightarrow B)}$  and  $P_{app(B\rightarrow A)}$ ) for analytes and Na-F, and efflux ratios (ER) for analytes obtained in the immortalized *in vitro* human BBB model based on hBMEC cell line (n = 3–4).

Compounds	Mean $P_{app} \pm SD$ ( $\times 10^{-6}$ cm/s)		Na-F: Mean $P_{app} \pm SD$ ( $\times 10^{-6}$ cm/s)		ER
	A→B	B→A	A→B	B→A	
Piperine	26.1 ± 0.986	34.2 ± 2.20	5.74 ± 0.0406	6.53 ± 0.703	1.31
SCT-66	7.25 ± 1.70	13.9 ± 2.59	6.28 ± 0.0369	6.28 ± 0.197	1.92
SCT-64	15.6 ± 0.480	11.7 ± 1.59	4.20 ± 0.372	4.84 ± 0.0928	0.750
SCT-29	3.38 ± 0.856	7.30 ± 0.675	4.51 ± 0.217	4.51 ± 0.0859	2.16
LAU397	3.55 ± 0.769	4.14 ± 1.43	4.91 ± 0.0298	4.59 ± 0.0287	1.16
LAU399	14.0 ± 4.90	16.8 ± 2.16	4.42 ± 0.135	5.07 ± 0.312	1.20

Na-F: sodium fluorescein; A: apical; B: basolateral

**Table S8** Mean apparent permeability coefficients ( $P_{app(A\rightarrow B)}$  and  $P_{app(B\rightarrow A)}$ ) for analytes and Na-F, and efflux ratios (ER) for analytes obtained in the *in vitro* human BLEC BBB model (n = 3).

Compounds	Mean $P_{app} \pm SD$ ( $\times 10^{-6}$ cm/s)		Na-F: Mean $P_{app} \pm SD$ ( $\times 10^{-6}$ cm/s)		ER
	A→B	B→A	A→B	B→A	
Piperine	25.1 ± 0.931	19.5 ± 3.08	8.53 ± 0.615	9.01 ± 0.483	0.777
SCT-66	11.7 ± 0.806	5.59 ± 0.331	9.44 ± 0.644	8.53 ± 0.132	0.478
SCT-64	11.2 ± 1.87	9.03 ± 0.590	8.02 ± 0.465	7.79 ± 0.254	0.804
SCT-29	3.31 ± 0.891	1.37 ± 0.153	9.86 ± 0.478	8.36 ± 0.438	0.414
LAU397	3.44 ± 1.03	1.40 ± 0.174	8.33 ± 0.356	8.29 ± 0.177	0.406
LAU399	5.69 ± 0.822	2.81 ± 0.202	9.87 ± 1.02	7.87 ± 0.614	0.493

Na-F: sodium fluorescein; A: apical; B: basolateral

**Table S9** Mean apparent permeability coefficients ( $P_{app(A\rightarrow B)}$  and  $P_{app(B\rightarrow A)}$ ) for analytes and Na-F, and efflux ratios (ER) for analytes obtained in the primary bovine endothelial/rat astrocytes co-culture *in vitro* BBB model (n = 3).

Compounds	Mean $P_{app} \pm SD$ ( $\times 10^{-6}$ cm/s)		Na-F: Mean $P_{app} \pm SD$ ( $\times 10^{-6}$ cm/s)		ER
	A→B	B→A	A→B	B→A	
Piperine	81.3 ± 2.04	32.2 ± 1.64	3.00 ± 1.12	0.731 ± 0.00699	0.396
SCT-66	27.9 ± 2.90	13.7 ± 0.830	3.88 ± 0.573	0.501 ± 0.0235	0.490
SCT-64	69.4 ± 7.40	27.9 ± 1.53	3.39 ± 0.530	0.779 ± 0.0207	0.402
SCT-29	20.9 ± 3.48	12.2 ± 1.54	5.07 ± 2.81	0.864 ± 0.0399	0.584
LAU397	38.0 ± 8.44	17.3 ± 1.00	3.42 ± 3.19	0.610 ± 0.0517	0.460
LAU399	44.8 ± 12.3	15.2 ± 0.440	2.15 ± 1.58	0.738 ± 0.239	0.340

Na-F: sodium fluorescein; A: apical; B: basolateral